



Dynamic studies of vortices in NbSe₂, from single flux lines to lattices

F. Pardo^{a,*}, C. Bolle^a, V. Aksyuk^a, E. Zeldov^a, P. Gammel^a, D.J. Bishop,
F. de la Cruz^b

^a Bell Labs Lucent Technologies, 600 Mountain Avenue, Murray Hill, NJ 07974, USA

^b Centro Atómico Bariloche CNEA, Bariloche, Argentina

Abstract

We present different techniques to study the dynamics of the vortex lattice in NbSe₂ single crystal samples. In the first set of experiments, we applied a field parallel to the *c* crystalline axis and extended the Bitter decoration technique to the study of dynamic structures by imaging the lattice during creep (“decoration during motion”). This method exposed a new smectic phase and an anisotropic “crystal” at higher fields. In the second set, we used a micro-mechanical high-*Q* oscillator to study the mesoscopic flux dynamics along the crystallographic *ab* plane. In this case, we were able to observe single vortex penetration, well described by a ‘1 + 1’-dimensional model. © 2000 Published by Elsevier Science B.V. All rights reserved.

Keywords: Vortices; Flux dynamics; Flux penetration; Flux lattice

1. Introduction

Several techniques exist to image the spatial magnetic structure of superconductors. Among them, the Bitter decoration technique emerges as single vortex resolution — large area technique widely used to study *static* properties of vortex lattices. In the first part of this paper, we show an extension of this powerful technique that allowed us to explore *dynamic* properties of the lattice by decorating during creep [1].

On the other hand, the study of the temporal behavior of individual vortices as they enter into the sample has also been hampered by the lack of suitable experimental tools, mainly for the mesoscopic regime, where a small number of vortices are con-

finied in a small volume. Here we used a polysilicon micromachined mechanical resonator to resolve the dynamics of single vortices in micrometer-sized samples [2]. These experiments are described in Section 2.

2. Dynamic decoration experiments

In the magnetic decoration technique used here, the flux line lattice (FLL) is visualized by evaporating ~ 50 Å magnetic particles onto the surface of a superconductor held below its transition temperature T_c with a magnetic field applied. The particles follow the field lines of the vortices at the surface of the sample and land where the vortices are located. Because each pile of magnetic particles has a finite size, the technique is limited to fields below several hundred oersteds. Fortunately, this range of fields

* Corresponding author.

covers an interesting region where we can tune the vortex interaction strength relative to the pinning strength and see a crossover from a moving Bragg glass in the high field, interaction-dominated limit, to a smectic structure in the low field, disorder-dominated limit.

Our samples were high-quality, single crystals of NbSe₂ with typical dimensions of $0.5 \times 0.5 \times 0.2$ mm³. Samples were cooled down to 4.2 K in a magnetic field applied in the *c* direction. At low

temperatures, the field was removed and the sample was decorated after a certain period of time.

With a 1 s decoration time, the behavior of the vortex velocity defines two regimes. If the velocity is greater than one vortex lattice constant per second, one has images of vortices in motion. For the regime of vortex velocities less than one lattice constant per second, one obtains quasi-static images of the slowly moving vortices. We can work in both regimes. Because of the critical state profile (independent of

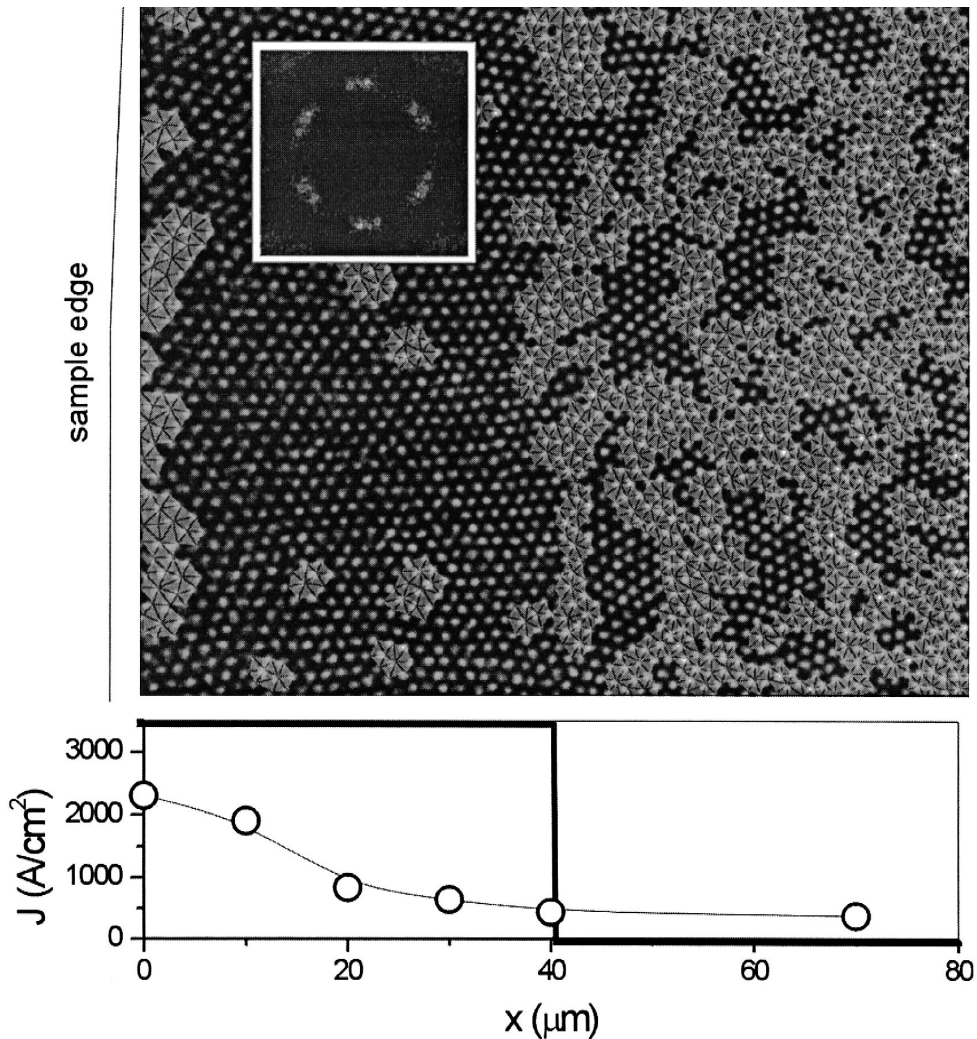


Fig. 1. Critical state during creep (quasistatic, 25 G), showing topological defects (clear areas). Fourier Transform in the ordered region, derived critical current profile and calculated beam profile for $J_c = 3500$ A/cm² [3].

velocity regime), we always find a quasi-static, homogeneous structure in the center of the sample and the critical state region at the edge. The data shown here are always from the critical state region.

2.1. Interaction-dominated regime

The large area picture of the critical state profile in the quasi-static regime shown in Fig. 1 is a clear example of motion-induced ordering of the FLL. The current distribution calculated from the field profile shows that in the critical state region, the FLL is much more ordered than in the center of the sample. The remaining topological defects (few percent in density) arise mainly because of the small field gradient. The Fourier Transform (FT) confirms this as one sees six well-defined peaks although there is still a one-dimensional modulation with two of the peaks brighter than the other four, indicating that the positional correlation length perpendicular to the flow direction is still longer than that parallel to the flow. These data suggest that the increased field allows the vortex–vortex interactions to dominate over the disorder and is the equivalent to turning down the disorder. The data are quite similar to the predicted moving Bragg glass phase [4,5].

For the data in the high-velocity regime, we found a pattern similar to that found in Refs. [7–9], showing coherent motion evidenced by large flow domains.

2.2. Disorder-dominated regime

Because the data in Fig. 2(A) are in the quasi-static regime, the image resolves individual vortices. This consists of rows of vortices aligned along the flow direction and not an isotropic, hexagonal pattern as would be seen for a static lattice. The FT data show the signature of a smectic phase [6]. The two sharp peaks show that the channels are well-ordered transverse to the flow of vortices and the broad lines of scattering show that the vortices are liquid-like in the channels with short-range positional correlations along the direction of flow.

The data in Fig. 2(B) are no longer in the quasi-static regime and the image no longer resolves individual vortices as clearly, but the same smectic pattern can be seen. A careful look at this image

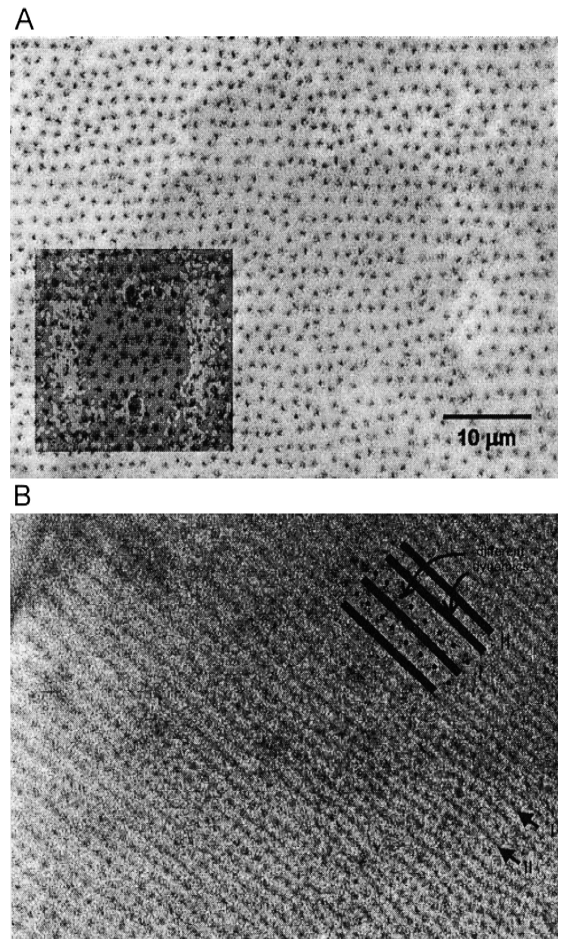


Fig. 2. Quasistatic decoration of the smectic structure (A) and (B) channels with different dynamics (decoupling) in the moving regime at 5 G.

reveals the existence of decoupled motion between channels: there are blurred and static channels.

3. High- Q micromechanical oscillator experiments

High- Q mechanical oscillators have previously been [7–9] shown to be powerful probes of condensed matter. However, the recent availability of silicon micromechanics has enormously expanded the power of the technique by allowing high Q and small size. Shown in Fig. 3 is a SEM micrograph of our micromachine. The mechanical oscillator con-

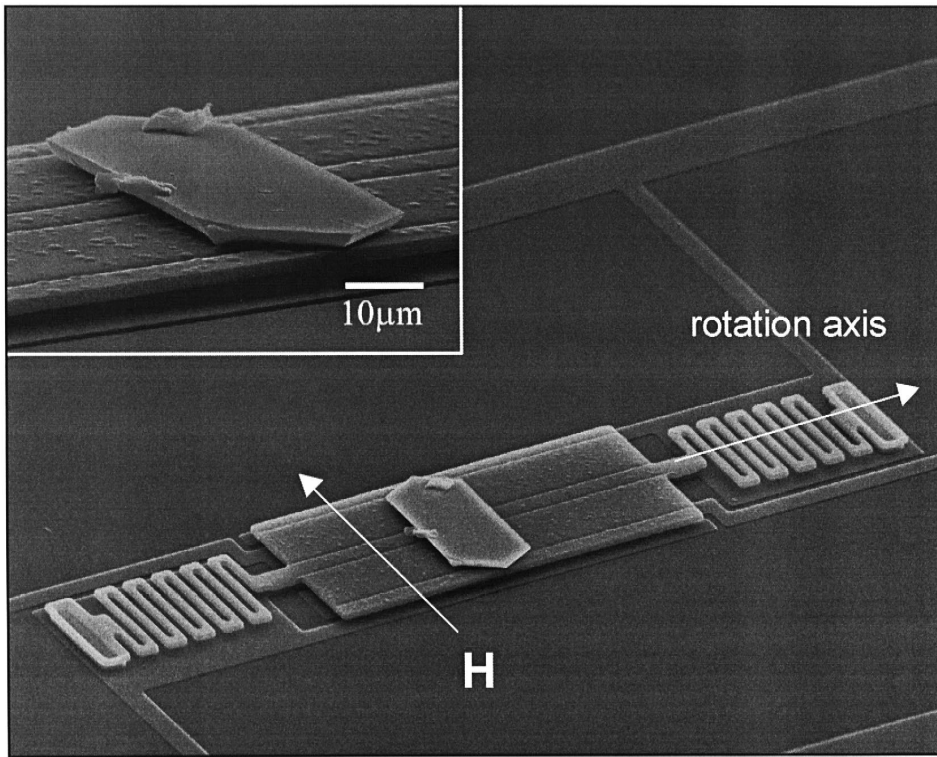


Fig. 3. SEM image of a high- Q mechanical oscillator with a hexagonally shaped single crystal mounted on top.

sists of a plate connected via two serpentine springs to two support structures attached to the substrate. Under the plate are two electrodes on the silicon substrate. The outline of the electrodes is visible on the top plate due to print through during the multiple processing steps. In operation, the device is oscillated torsionally about the long axis of the plate. One electrode is used to drive the plate and the other to detect the actual movement. This torsional mode has a resonant frequency of 45 kHz and a Q of 250,000 at low temperatures. The device was built using a three-layer polysilicon process at the MCNC MUMPs foundry [10].

Shown in the inset to Fig. 3 is a blowup of the sample used for the studies described here. It is a single crystal with dimensions of $22 \times 49 \times 1.6 \mu\text{m}^3$ with a T_c of 7.0 K.

A magnetic field was applied parallel to the large face of the crystal and perpendicular to its rotation axis. A sample with a magnetic moment \vec{M} in a field \vec{H} exerts an additional torque $\tau = \vec{M} \times \vec{H}$ on the

oscillator, shifting its resonant frequency. The small size of the oscillator allows us to obtain high resonant frequencies despite the soft spring constants, typically in the range of 0.5×10^{-9} N m.

Shown in Fig. 4 is the frequency and amplitude dependence for a standard ZFC–FC temperature sweep. After applying a field of 60 Oe at 5 K, we observe a frequency shift of roughly 20 Hz and no change in the oscillator's amplitude. This is a clear signature of the Meissner state. The energy cost of screening a magnetic field applied parallel to the face of a thin superconductor is smaller than the cost of screening the same field applied perpendicular to the face of the sample. The resulting variation of the torque with the tilt angle $d\tau/d\theta$ causes a restoring force that increases the oscillator frequency. The result is an *increase* in the oscillator frequency with no change in the amplitude (no dissipation). As we warm up the sample (solid line), we do see a slight decrease in the Meissner restoring force as $\lambda(T)$ starts to become comparable to the sample thickness.

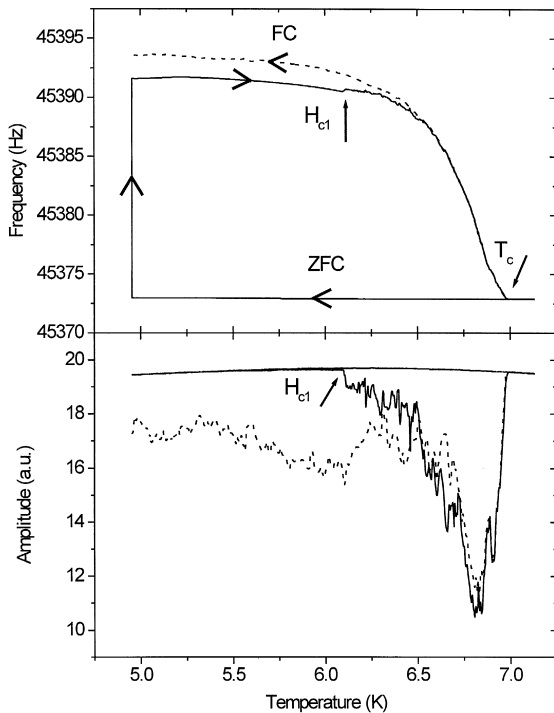


Fig. 4. Temperature dependence of the oscillator resonant frequency (top) and amplitude (bottom) for a typical zero field cooling–field cooling (ZFC–FC) experiment.

At $T \approx 6.1$ K, we see a sudden drop in the oscillator amplitude and a jump in its frequency. These changes are associated with the first flux line penetration and uniquely define the location of the first penetration field $H_p \approx H_{C1}$ for our sample. Note the increase in the “noise” in the data that, as we show below, is the resolution of single vortex events in the oscillator. As we approach T_c , both the frequency and the amplitude merge into the background. Upon cooling the sample (dashed line) in the presence of the 60 Oe field, the flux lines nucleate in the superconductor below T_c , resulting in a frequency shift and a decrease in amplitude (increase in dissipation). Both the frequency and the amplitude show a rich structure close to T_c that tends to smooth out at lower temperatures. This structure represents the changes in the pinning strength of the vortex ensemble as the number of flux lines changes.

Shown in Fig. 5(a) is a field sweep close to T_c after a ZFC. The frequency shift in the Meissner state due to the shielding currents up to $H_{C1} \approx 9$ Oe

has the expected H^2 dependence. Above H_{C1} , we see a series of peaks in the frequency that we interpret as the signature of the first several flux lines entering the sample. The field scale and the size of the sample are consistent with this interpretation. The first flux lines that go into the sample wander significantly away from the field direction to take advantage of the point disorder. As the field increases, more lines enter the sample and these wandering lines start to interact. Fig. 5(b) shows the response at a lower temperature ZFC field sweep. The Meissner regime once again is quadratic, but the penetration of single vortices above H_{C1} is somewhat different due to the stronger effects of pinning at lower temperatures. At this temperature, as the individual vortices enter, there are mesas between the jumps. If the field is cycled back and forth a fraction of an oersted, the response in the mesas is reversible, but the jumps are not. The reason for the non-monotonic behavior with increasing field is the

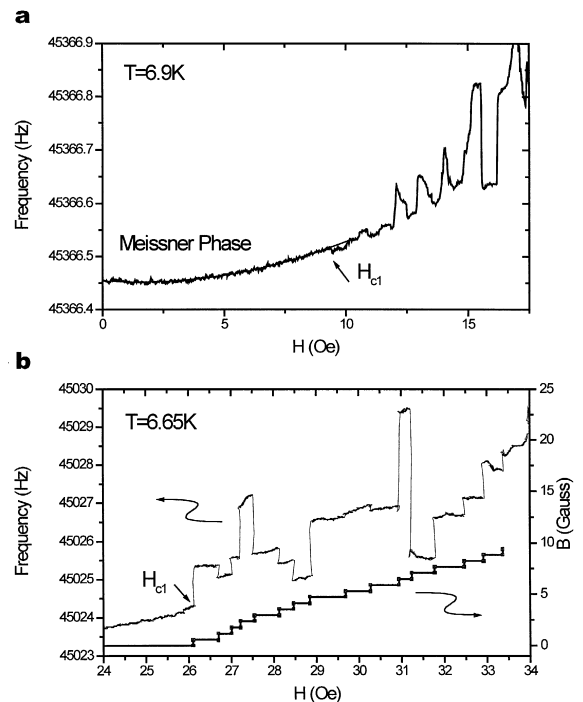


Fig. 5. Different field dependencies of the resonant frequency at fixed temperatures: (a) individual vortex penetration, (b) reversible mesas separated by irreversible jumps, associated with a single flux line entering the sample. The lower trace is $B(H)$ extracted by counting vortices.

mesoscopic nature of our system. As the vortices enter the sample, sometimes it means that the entire ensemble is better pinned and the frequency increases, but sometimes, because of interactions, it is less well pinned and the frequency decreases. The lower trace is $B(H)$ extracted from the data by counting vortices. In this case for $N(H)$ flux lines in the sample and a sample cross-section area $S = 22 \times 1.6 \mu\text{m}^2$, we have $B \approx N(H)\Phi_0/S$. The data are a discrete approximation to the continuum prediction of a *linear* $B(H)$ near H_{Cl} , consistent with point disorder in 1 + 1 dimensions [4,5]. This result is in striking contrast to the vertical slope predicted by Abrikosov's original theory of perfectly straight vortices in clean samples with exponential repulsion.

Taken together, Figs. 4 and 5 provide evidence of the mesoscopic behavior of a small number of vortices in a finite-sized sample where the details of the pinning sites produce sample-specific structure in the magnetization of the superconductor.

References

- [1] F. Pardo, F. de la Cruz, P.L. Gammel, E. Bucher, D.J. Bishop, Nature 396 (1998) 348.
- [2] C.A. Bolle, V. Aksyuk, F. Pardo, P.L. Gammel, E. Zeldov, E. Bucher, R. Boie, D.J. Bishop, D.R. Nelson, Nature 399 (1999) 43.
- [3] F. Pardo, D.J. Bishop, P.L. Gammel, F. de la Cruz, Proceedings of IWCC9, Madison, WI, USA, July 1999,1999.
- [4] I.T. Giarmarchi, P. Le Doussal, Phys. Rev. Lett. 76 (1996) 3408.
- [5] P. Le Doussal, T. Giarmarchi, Phys. Rev. B 57 (1998) 11356.
- [6] L. Balents, M.C. Marchetti, L. Radzihovsky, Phys. Rev. B 57 (1998) 7705.
- [7] R.N. Kleiman, G. Agnolet, D.J. Bishop, Phys. Rev. Lett. 59 (1987) 2079.
- [8] R.N. Kleiman, G.K. Kaminsky, J.D. Reppy, R. Pindak, D.J. Bishop, Rev. Sci. Instrum. 56 (1985) 2088.
- [9] D.J. Bishop, J.D. Reppy, Phys. Rev. Lett. 40 (1978) 1727.
- [10] <http://www.mcnc.org>.